Wind Tunnel Measurements of the Response of Hot-Wire Liquid Water Content Instruments to Large Droplets

J. W. STRAPP,* J. OLDENBURG,+ R. IDE,+ L. LILIE,# S. BACIC,* Z. VUKOVIC,* M. OLESKIW,@ D. MILLER,+ E. EMERY,+ AND G. LEONE&

*Meteorological Service of Canada, Downsview, Ontario, Canada
+NASA Glenn Research Center, Cleveland, Ohio
#Science Engineering Associates, Mansfield Center, Connecticut
@National Research Council of Canada, Ottawa, Ontario, Canada
&Centro Italiano Ricerche Aerospaziali, Capua, Italy

(Manuscript received 6 May 2002, in final form 6 December 2002)

ABSTRACT

Wet wind tunnel tests were performed on more than 23 cloud liquid water content (LWC) probes and drop spectrometers at the NASA Icing Research Tunnel, with a main objective to characterize their response to large-droplet conditions. As a part of this study, the LWC and median volume diameter (MVD) reference values of the tunnel were examined, and accuracies were estimated and reported herein. Alternative MVDs were calculated from measurements conducted during the study. MVD accuracy was particularly difficult to estimate due to the lack of accepted standards, and MVD estimates were quite sensitive to the complement of instruments used to generate composite droplet spectra.

Four hot-wire LWC probes were tested to characterize the LWC response as a function of cloud MVD. A response reduction was observed with increasing MVD for all three probes with cylindrical hot wires, most significant for the probe with the smallest wire diameter. The response of the Nevzorov total water content (TWC) probe, with its relatively large-diameter conical hot wire, did not roll off appreciably within the range of MVDs tested, although significantly larger inertial collision efficiency corrections were predicted for smaller droplets. The results corroborate previous studies that suggest re-entrainment of collected water likely creates a rolloff of the response of small-diameter cylindrical hot-wire probes, but also suggest that the aerodynamic design of the Nevzorov TWC probe inhibits re-entrainment by trapping droplets that enter its sample volume.

1. Introduction

Since the 1950s, hot-wire probes have been the most commonly used devices to estimate cloud liquid water content (LWC) from research aircraft. The first popular device was the Johnson–Williams (JW) probe (Neel 1955), which deduced cloud LWC by the change in electrical current of a heated cylindrical hot wire at constant voltage as it cooled due to evaporation of cloud droplets. In the early 1980s, Particle Measuring Systems (PMS) began production of a constant-temperature hot-wire device, hereafter called the ''King'' probe, using a design described by King et al. (1978). The main advantage of the constant-temperature device was that the response characteristics were, for the most part, fully calculable and described from first principles, and in theory an independent calibration was not required. Although other hot-wire devices have been developed and reported (e.g., Merceret and Schricker 1975; Nevzorov 1980; Korolev et al. 1998b), the JW and King probes have been the most commonly used on research aircraft and in tunnels over the last few decades.

The nominal wire diameters of the JW and PMS King probe are 0.56 and 1.85 mm, respectively. There is a known decrease in collision efficiency with decreasing droplet size dependent on the wire diameter. Calculations of Finstad et al. (1988) reveal that collision efficiencies at a typical aircraft speed of 100 m s^{-1} and a typical pressure of 70 kPa rapidly drop below 0.9 for droplets smaller than about 9- and 12-μm diameter for the JW and King probes, respectively. However, other investigators have discovered that the response of cylindrical hot-wire devices also drops off with increasing drop size. Owens (1957) determined a limit in the drop diameter of approximately 30 μm for the JW, above which partial aerodynamic removal of captured water mass before full evaporation was hypothesized. Spyers-Duran (1968) compared JW and replicator LWC measurements, and also inferred that the response of the JW probe decreased for water droplets larger than 30 μm. Biter et al. (1987) characterized the decrease in response

Corresponding author address: J. W. Strapp, Cloud Physics Research Division, Meteorological Service of Canada, 4905 Dufferin St., Downsview, ON M3H ST4, Canada.
E-mail: Walter.Strapp@ec.gc.ca

TABLE 1. Summary of instruments tested at the NASA IRT during this experiment.

Hot-wire LWC probes	Conventional particle spectrometers	Others
PMS King	PMS FSSP (3–45, 5–95 μm)	Airborne PVM-100A
Johnson–Williams	PDPA (2–120 μm)	Rosemount ice detector
Nevzorov LWC/TWC	PDPA (80–2000 μm)	SPEC Cloud droplet spectrometer (CDS)
Prototype Nevzorov LWC/TWC, King-type electronics	PMS 2DC (25–800 μm)	NCAR counterflow virtual impactor (CVI)
Prototype Johnson–Williams constant-temperature wire	PMS 2D2C (25–800 μm)	NASA icing blade
	PMS 2DC gray (15–960 μm)	NRC rotating icing cylinder
	PMS 2DC gray (25–1600 μm)	
	PMS 1D230X (15–450 μm)	
	PMS 1D260X (10–600 μm)	
	PMS 1DP (50–1500 μm)	
	PMS 2DP (200–6400 μm)	
	SPEC CPI (2.3–2000 μm)	

of the PMS King probe with increasing median volume diameter (MVD). Therefore, not only is there a significant known rapid response rolloff as drop diameter decreases below about 12 μm, but there is an additional response rolloff as drop size increases that is not as well characterized, and the cause of which has not been precisely described.

Since the mid-1990s, there has been an increased interest in characterizing natural clouds containing supercooled large drops (SLDs), due to the fatal accident involving an ATR-72 aircraft over Roselawn, Indiana, on 31 October 1994. Due to potential aircraft icing certification implications, there is a strong interest in understanding the response and accuracy of our primary cloud measurement devices under such conditions. Furthermore, a new production aircraft hot-wire research device, the Nevzorov LWC/total water content (TWC) probe, has been in more common use over the past seven years (Korolev et al. 1998b) with wire geometry characteristics that are postulated be more favorable to large drop measurement. The purpose of this article, therefore, is to assess the response of the JW, PMS King, and Nevzorov LWC and TWC devices in large droplet conditions, using a large calibrated wet wind tunnel.

2. The experiment conducted at the NASA Icing Research Tunnel

During the period of 21 September–9 October 1998, the Meteorological Service of Canada (MSC) and the National Aeronautic and Space Administration (NASA) Glenn Research Center collaborated on a 3-week wind tunnel investigation of the performance of common aircraft cloud physics probes in large droplet conditions. A list of the tested probes is given in Table 1. These included an array of cloud particle spectrometers, hot-wire devices, and several less common instruments or prototype devices. In addition to the MSC and NASA, test participants included a variety of agencies and private companies from North America and Europe. The results of testing of the Gerber Scientific airborne Particle Volume Monitor model PVM-100A and the counterflow virtual impactor (CVI) have been summarized by Wendisch et al. (2002) and Twohy et al. (2003), respectively.

The NASA Icing Research Tunnel (IRT) is a large wet wind tunnel with a sample cross section approximately 2 m high by 3 m wide. For these tests, spray was injected into the tunnel through more than 100 nozzles distributed across 10 horizontal spray bars. NASA measured the LWC gradients resulting from this array of nozzles using large icing screens and produced LWC spatial contours for many of the conditions used in this study. These were used to identify two primary locations near the center of the tunnel with negligible LWC difference to allow simultaneous testing of two probes. An additional position was chosen for a dedicated PMS King probe in a failed attempt to measure tunnel LWC repeatability; analysis would later show that this location was not representative of the primary locations. Figure 1 displays the instrument configuration in the tunnel for one of the experiments of this study.

The spray LWC and MVD are controlled by varying the nozzle water and air pressures. Their ranges are interdependent, but for these tests they varied between approximately 0.23 and 1.4 g m^{-3} for LWC, and nominally (from past NASA calibrations) 16–270 μm for MVD. The test matrix (Table 2) was designed to provide both a series of probe LWC calibrations at nominally constant MVDs of 16 and 40 μm (''LWC sweeps''), and a series of calibrations at roughly constant LWC varying the MVD from nominally 16 to 270 μm (''MVD sweeps''). Measurements described in section 3 provide an alternative set of MVDs adopted for this study, where the 16-μm LWC sweeps have been renamed ''low MVD range LWC sweeps (12.9–17.6 μm)'' and the 40-μm LWC sweeps have been renamed ''intermediate MVD range LWC sweeps (29.5–32.5 μm).'' The MVD sweeps have been redefined to span 12.9–236 μm. Airspeeds of 67 and 100 m s^{-1} were chosen for testing, representative of the NASA Twin Otter and NRC Convair 580 aircraft typical operating airspeeds. The ranges shown

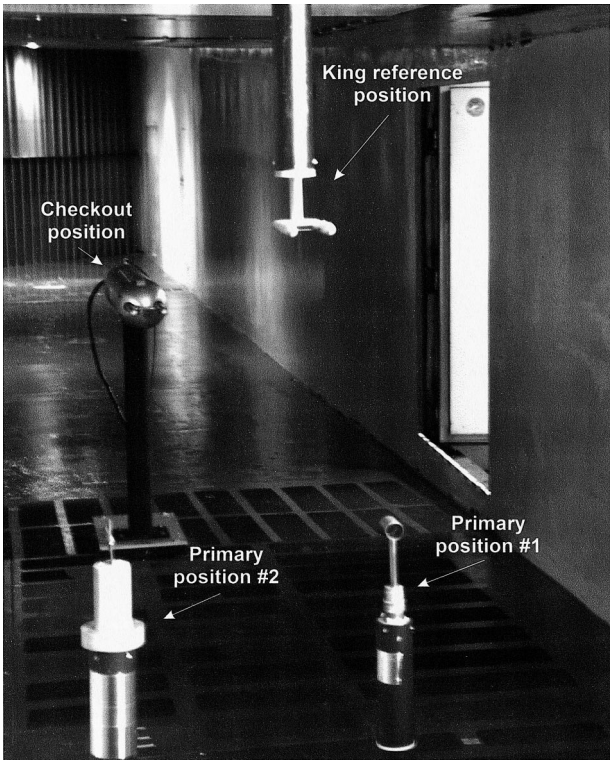

FIG. 1. Test section in the NASA IRT during the Sep–Oct 1998 testing, showing the two primary calibrations positions in the central uniform LWC region of the tunnel, the PMS King reference position intended for repeatability measurements, and a rear checkout position for instrument debugging.

in Table 2 represent a best attempt to cover as much as might be typically observed in natural clouds within the constraints of the tunnel. The most notable deficiency of the test matrix is the lack of low LWCs that are common in natural clouds.

All instruments were tested at either of the two primary test locations under the same conditions shown in Table 2. Due to operational problems or known probe limitations, not all test points were achieved or even attempted for all instruments. However, a total of more than 800 test points were accomplished over 15 test days. The hot-wire results represent approximately one-quarter of the measurements made during the study.

3. The IRT calibration

Reference values of the LWC and MVD for each test point are available from past calibrations at the IRT. In this section, the tunnel LWC and MVD reference values will be examined and compared to the results from other methods, and attempts will be made to estimate their accuracy. Standard NASA reference LWC values for MVDs smaller than 34 μm will be adopted in this article, but an alternative set of LWCs will be substituted for MVDs larger than 34 μm, and an alternative set of MVD values will also be substituted. Standard NASA MVDs will hereafter be referred to as NASA MVDs, and the substituted set from this study will be referred to as study MVDs. These revised LWC and MVD values are also used by Wendisch et al. (2002) and Twohy et al. (2003).

a. Tunnel LWC reference values

NASA derives its reference LWC from icing blade measurements when the NASA MVD is less than 50 μm, and from a large diameter (3.8 cm) rotating icing cylinder for larger MVDs. This corresponds to a study MVD changeover point of approximately 34 μm. Test conditions with study MVDs less than and greater than or equal to 34 μm will hereafter be referred to as small-droplet (SD) and large-droplet (LD) conditions, respectively. The absolute accuracy of SD icing blade reference values has not been directly reported in the literature, although a rough estimate can be made from previous studies. LWC is derived from measurements of the thickness of ice accreted on a 3.2-mm-wide icing blade for a measured amount of time (Ide and Oldenburg 2001). This method is similar to the small-diameter (2.42 mm) rotating icing cylinder measurement used as an LWC reference at the National Research Council (NRC) Altitude Icing Wind Tunnel (AIWT; Oleskiw et al. 2001). Stallabrass (1978) has analyzed the potential sources of errors in the NRC rotating icing cylinder LWC calculation, estimating the effects of assumptions of ice density, constant collection efficiency as the cylinder grows due to ice accretion, droplet size, and several other factors on absolute accuracy. Clearly some assumptions and measurement biases can lead to quasi-fixed-scale-factor errors that could lead to consistent LWC overestimation or underestimation. Stallabrass concluded that most errors were of the order of a few percent, and some error cancellation was likely. Although no final absolute error estimate was provided, the implication was that the absolute accuracy was within a few percent. Stallabrass also compared their rotating icing cylinder to an icing blade similar to that used by NASA, finding agreement to within a few percent, thereby implying that the icing blade absolute accuracy was also within a few percent. NASA uses the large-diameter rotating icing cylinder as a reference for LD test points because it is presumably less sensitive to drop splashing and re-entrainment suspected in conventional narrow icing blade and icing cylinder measurements. Standard tunnel LD LWC calibrations had been performed in the past at speeds of 56, 73, and 87 m s^{-1}. For the purposes of these tests, LD LWCs were estimated at 67 and 100 m s^{-1} by scaling the former results, and were adjusted for the collection efficiencies corresponding to the study MVDs. The absolute accuracy of the LD rotating cylinder method for large MVD sprays has not been reported but has been estimated by NASA to be 20%.

Due to the cold temperatures and relatively long time required for icing blade or cylinder measurements, it is

TABLE 2. Test matrix points used for this experiment. NASA MVDs are derived from their past FSSP, 1D230X, and 1DP measurements. The study MVDs are those measured by the PDPA, 2DC, and 2DP probes, and are those adopted for this study. PDPA data were not available for all data at 100 m s^{-1}, but since the same nozzle air and water pressures were used for the LWC sweeps at both airspeeds, the MVDs at 100 m s^{-1} are expected to be similar to those at 67 m s^{-1}.

67 m s^{-1}					100 m s^{-1}				
Condition no.	NASA LWC (g m^{-3})	Study LWC (g m^{-3})	NASA NVD (μm)	Study MVD (μm)	Condition no.	NASA LWC (g m^{-3})	Study LWC (g m^{-3})	NASA MVD (μm)	Study MVD (μm)
Low MVD LWC sweep					Low MVD LWC sweep				
121	0.32	0.32	16	17.3	31	0.23	0.23	16	n/a
22	0.40	0.40	16	17.6	32	0.29	0.29	16	n/a
23	0.50	0.50	16	16.8	33	0.36	0.36	16	n/a
24	0.60	0.60	16	15.2	34	0.46	0.46	16	n/a
25	0.70	0.70	16	12.9	35	0.51	0.51	16	n/a
12	0.70	0.70	16	15.1	2	0.60	0.60	16	13.4
Intermediate MVD LWC sweep					Intermediate MVD LWC sweep				
26	0.64	0.64	40	29.5	36	0.47	0.47	40	n/a
15	0.70	0.70	40	30.8	37	0.62	0.62	40	n/a
27	0.85	0.85	40	31.4	5	0.70	0.70	40	31.9
28	1.03	1.03	40	30.0	38	0.75	0.75	40	n/a
29	1.21	1.21	40	31.5	39	0.88	0.88	40	n/a
30	1.41	1.41	40	32.5	40	1.03	1.03	40	n/a
MVD sweep, 0.7–1.01 g m^{-3}					MVD sweep, 0.54–0.77 g m^{-3}				
12	0.70	0.70	16	15.1	2	0.60	0.60	16	13.4
25	0.70	0.70	16	12.9	104	0.70	0.70	18	14.7
101	0.70	0.70	18	17.3	3	0.70	0.70	20	21.8
13	0.70	0.70	20	21.2	105	0.70	0.70	25	27.7
102	0.70	0.70	25	24.2	4	0.70	0.70	30	29.5
14	0.70	0.70	30	28.4	106	0.70	0.70	35	n/a
103	0.70	0.70	35	n/a	5	0.70	0.70	40	31.9
15	0.70	0.70	40	30.8	6	0.70	0.76	50	36.3
16	0.70	0.78	50	34.2	7	0.47	0.54	70	35.0
17	0.70	0.84	70	33.9	8	0.48	0.55	100	41.1
18	0.70	0.77	100	50.8	9	0.48	0.54	120	47.1
19	0.75	0.83	120	57.0	10	0.74	0.77	175	96.4
20	0.96	0.97	175	128.6	11	0.75	0.76	270	236.4
21	1.00	1.01	270	216.3					

usually not practical to perform these measurements each time a probe is tested at the IRT. Instead, the tunnel calibration is established from a dedicated series of measurements, and empirical equations are derived to relate the tunnel LWC (at the center of the tunnel) to nozzle air pressure, the difference between water and air pressure, and tunnel velocity (Ide and Oldenburg 2001). Therefore, it is assumed that recreating tunnel nozzle settings reproduces LWC values with an acceptable level of accuracy relative to the reference calibrations. Random LWC variations from the established tunnel calibration thus enter into the estimate of absolute accuracy for any specific test run.

Icing blade and rotating icing cylinder measurements were made in both of the primary locations for a representative subset of the test matrix points listed in Table 2. These tests allow for a limited recheck of the tunnel LWC parameterizations, a direct comparison of the tunnel reference LWC methods of the NASA IRT and the NRC AIWT, a direct measurement of the expected difference in LWC between the two primary locations, and an estimation of the expected dispersion of the LWC due to tunnel random variations. A comparison of the SD LWCs measured at the two primary locations revealed only small and perhaps insignificant differences. Both the blade and cylinder regressions through the origin, location 1 versus location 2, yielded slopes of about 1.02. Figure 2 shows a comparison of blade and cylinder measurements to the standard NASA LWC parameterization. Examining the SD data points, most lie near and around the one-to-one line. Larger differences are seen for the LD points, because the tunnel reference LWC is determined with the large rotating cylinder for these points. The regression forced through the origin for the SD blade data has a slope of 0.998, indicating that the NASA LWC calibration has been essentially duplicated and suggesting that the SD LWC calibration did not change appreciably with time. The corresponding slope for the NRC icing cylinder LWC data is 1.039, indicating that the NRC reference method yields on the average 4% higher values than the historical NASA tunnel reference. A direct comparison of the NASA blade and AIWT icing cylinder SD results at the same primary location (taken 1 day apart) also shows icing cylinder

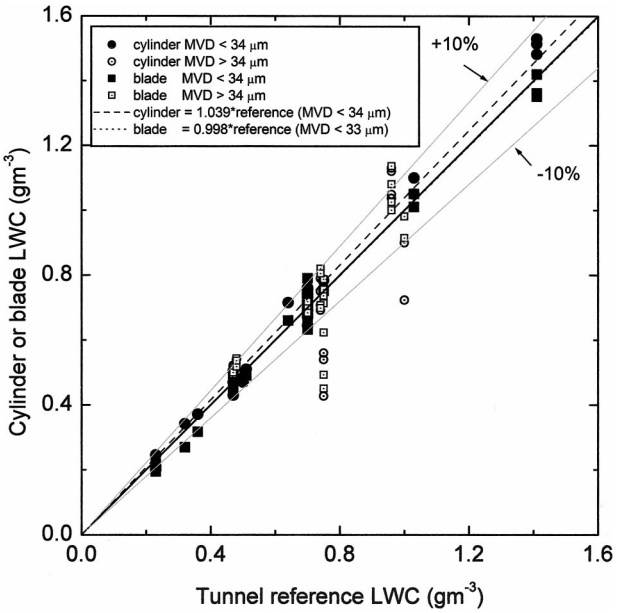

FIG. 2. Results of measurements during this study of the NASA IRT and NRC AIWT LWC reference methods (icing blade and small rotating icing cylinder, respectively) to the earlier derived tunnel reference LWC calibration parameterization. Small droplet (<34-μm study MVD) and large droplet (>34-μm study MVD) points are shown as solid and hollow points, respectively. A larger rotating cylinder is used to derive tunnel reference LWCs for study MVDs >34 μm due to suspected splashing.

values about 4% higher than icing blade values. Note that the scatter in the individual SD comparisons in Fig. 2 is contained between $\pm$10% of the one-to-one line. This is a reflection of the tunnel variability, presumably resulting from turbulence and small random migrations of the tunnel LWC spatial distribution pattern with time. The actual dispersion of the tunnel could be carefully determined by calculating the statistics for a large number of icing blade repeats at each condition. However, due to time constraints, only a limited number of repeats were conducted for the icing blade and small-diameter icing cylinder measurements in this study. The results showed an average repeat absolute difference of 3.5%, with maximum differences of about $\pm$8%. For normally distributed errors, this average absolute difference statistic can be empirically shown to be approximately equal to the average dispersion.

These observations have been combined into a rough estimate of the reference LWC absolute accuracy. For SD conditions, the absolute error estimates of a few percent by Stallabrass (1978) for the icing cylinder, consistent with the observations above of a small 4% bias between blade and cylinder, and the possible small bias between positions 1 and 2, have been combined and rounded into a rough overall accuracy in the scaling of the reference LWC values of $\pm$5%. An additional dispersion for individual test points of approximately 3.5% can be expected due to tunnel random variations. So, for example, comparisons of instrument measurements to tunnel reference LWC with regression slopes between 0.95 and 1.05 would not be considered significantly different from tunnel reference values. Tunnel LWC dispersion estimates would further predict that 95% of the points should lie between $\pm$7% ($\pm 2\sigma$) of those regression lines. For LD conditions, uncertainties in MVDs alone lead to uncertainties of up to 15%, and splashing effects are essentially unknown. The NASA LWC error estimate of $\pm$20% will be adopted for this study due to lack of further information, although it is acknowledged that it could be higher.

b. Tunnel MVD reference values

The standard NASA MVD reference values are derived from composite particle spectra of the NASA PMS forward scattering spectrometer probe (FSSP) (3–45 μm), ID230X (15–450 μm), and IDP (50–1500 μm) probes. NASA performs these calibrations at one tunnel velocity only, as has been recommended to the Society of Automotive Engineers by an FAA working group as an acceptable practice for calibration and acceptance of icing wind tunnels. NASA formulates these results into equations relating MVD to nozzle air pressure, and water–air differential pressure only.

Due to the large number of probes tested during this experiment (Table 1), it was possible to consider a variety of combinations of probes from which to construct a composite particle spectrum. In this section, the alternative choice of MVD adopted for this study (the study MVD) is described. This study MVD was derived from composite spectra using the instruments that were felt to be the most technically defendable in view of the testing done during this experiment [the phase Doppler particle analyzer (PDPA), MSC 2DC, and MSC 2DP probes]. Comparisons are made to the NASA MVD reference.

The PMS FSSP is the most commonly used small droplet–measuring device for most airborne natural cloud studies. However, the wind tunnel is a particularly challenging environment in which to make accurate FSSP measurements. During these tests, measurements were attempted using a number of FSSPs, but flawed and inconsistent data were obtained due to inadequate probe anti-icing and fogging. After much remedial effort, some stable results were finally obtained at 67 m s^{-1}, but no useful data were ever collected at 100 m s^{-1}. Furthermore, clouds produced by nozzles such as those used in the NASA IRT are distinctly different from those of natural clouds, with broad distributions with high concentrations of small droplets, and little evidence of a spectrum mode often seen in natural clouds. For example, the total concentrations of droplets for the low MVD sweep at 67 m s^{-1} varied between 530 and 2050 cm^{-3}, with typically 85% of the particles smaller than 10 μm. FSSP activities during many of the test conditions exceeded 50% and sometimes reached 90%. The

TABLE 3. Additional information on PMS OAPs tested at the IRT. The photodiode spacing is denoted by Δd. The 2D gray probes have the option to image particles with a minimum of 1 diode at the 50% or 75% shadow level; the 50% option was used for these tests. The 1D probes require at least one photodiode registration at the 66% level.

Probe	Model no.	Name	No. of diodes	Δd (μm)	Shadow level(s)
2DC	OAP-2D-C	Two-dimensional cloud droplet probe	32	25	50%
2D2C	OAP-2D2-C	Two-dimensional cloud droplet probe	32	25	50%
2DC gray	OAP-2D-GA2	Two-dimensional grayscale droplet probe	64	25	25%, 50%, 75%
2DC gray	OAP-2D-GA2	Two-dimensional grayscale droplet probe	64	15	25%, 50%, 75%
2DP	OAP-2D-P	Two-dimensional precipitation probe	32	200	50%
1D230X	OAP-230X	One-dimensional optical array cloud droplet probe	30	15	50%
1D260X	OAP-260X	One-dimensional optical array cloud droplet probe	62	10	50%
1DP	OAP-200Y	One-dimensional optical array precipitation probe	30	50	50%

activity is a measurement of the time the FSSP is busy sampling and processing particle detections. High activity percentages are related in a nonlinear fashion to undercounting due to particle coincidences and dead time (Baumgardner et al. 1985; Brenguier and Amodei 1989; Brenguier 1989; Breguier et al. 1994). Comparisons of FSSP LWC, corrected for coincidence and dead time losses, and tunnel LWC for SD conditions generally were strongly nonlinear, with acceptable agreement at low LWC and low activities, but with FSSP LWC exceeding tunnel values by more than a factor of 2 as LWC and activity increased. This behavior is symptomatic of droplet oversizing due to coincidences (Cooper 1988). In order to partially address this problem in earlier calibrations, NASA had performed some of their standard MVD calibrations with half the number of nozzles to reduce drop concentrations, but they still observed high FSSP activities for many test points. In contrast, the airborne PDPA, measuring droplet spectra in the 2–120-μm size range with a size resolution of 0.4 μm, provided excellent deicing, no evidence of fogging, and linear comparisons of spectrum integrated SD LWC to tunnel LWC. It was calibrated onsite by a representative of the manufacturer, who also supervised the collection of data. The PDPA determines particle size by examining fringe patterns in the far field produced by particle light scattering within two intersecting lasers. Particle sizing is not very sensitive to optical contamination such as fogging. Coincident particles in the sample volume are rejected and cannot lead to the coincidence oversizing suspected for the FSSP. Rudoff et al. (1993) performed an earlier series of tests at the NASA IRT, obtaining a very linear relationship between the icing blade and PDPA LWC, with a slope of 1.00, and a standard deviation of 0.13. This is a strong testament to the sizing capability of the probe within the small droplet size region, in contrast to observations of the FSSP. The designer of the PDPA tested in the IRT (W. Bachalo 2002, personal communication) has estimated its absolute MVD accuracy as approximately $\pm 10\%$ for MVDs < 40 μm and indicated that sample volume was more of a problematic issue than sizing. During the present tests at 67 m s^{-1}, a linear relationship was again found between the PDPA and tunnel LWC, but PDPA LWC was found to be lower than tunnel LWC. It was concluded that this was a correctable sample volume error that varied with airspeed, which could be largely accounted for by the fraction of particles accepted by the probe. Particles are rejected in the standard PDPA software if their optical signature does not adequately match that expected for a sphere. Such registrations are considered to be noise, and no correction is applied to concentrations. In this study, the average ratios of PDPA LWC to tunnel LWC for SD conditions were 0.63 and 0.26 at 67 and 100 m s^{-1}, respectively, while the corresponding ratios of accepted to total particles were 0.65 and 0.33. The similarity of these ratios suggests that real particle rejections may explain why the PDPA LWCs were low by an airspeed-dependent scale factor. Regardless of the cause, the PDPA concentrations have been adjusted by a scale factor of 1.6 and 3.88 at 67 and 100 m s^{-1} assuming LWC differences are due to a correctable sample volume error.

Since the PDPA does not provide data past 120 μm, and has a relatively small sample volume for large droplet sampling, the data from the different optical array probes (OAPs) in Table 1 were examined in order to provide measurements of the higher size range. Table 3 displays some details of these probes. The 2DC probe utilized in the IRT incorporated the faster photodetector array (Silicon Detector Corporation) used in later OAPs. The 2D2C probe is a more recent version of the 2DC with random access memory instead of shift registers. In general, the family of 1D probes has the advantage of simpler data processing, but the images and interarrival times provided by 2D probes allow for some phase discrimination and artifact rejection, and thus a higher confidence in spectrum fidelity. All OAPs suffer from sizing and counting errors, due to out-of-focus missizing, digitization, and time response (e.g., Reuter and Bakan 1998; Korolev et al. 1998a; Baumgardner and Korolev 1997; Strapp et al. 2001; Jensen and Granek 2002). Efforts to apply data corrections by several of these authors have not fully resolved problems. Strapp et al. (2001) characterized the size response of the 2DC used in this study using rotating reticles with spots of known diameters. They showed that spectrum errors predicted for the constant depth-of-field part of

the size spectrum are relatively small, but missizing of droplets smaller than about 100 μm, whose depth-of-field values vary rapidly with size, can create large spectrum uncertainties in this size region. Their arguments extend in general terms to all of the OAPs listed in Table 3. The more recently developed Stratton Park Engineering Company Cloud Particle Imager (CPI, Table 1) provides high-resolution (2.3 μm) images of particles and shows promise in providing the quantitative estimates of particle spectra and phase below 100 μm that are currently needed (Lawson et al. 2001). All probes may also suffer from some degree of artifact contamination due to splashing of droplets off the probe surfaces ahead of the sample volume (Jensen and Granek 2002). The degree of contamination is somewhat of an open question at this time, as there has been little physical study of this effect. Figure 3a shows a comparison of particle spectra measured by several probes during the IRT testing. An in-depth analysis of the differences observed in Fig. 3 is beyond the scope and practical limitations of this article. For simplicity, no corrections have been applied to the spectra, and 2D gray data have been interpreted in a manner identical to a single shadow-level 2DC probe. Channel sizes and sample areas listed in the probe manuals were used. Note that above approximately 50 μm, the 2DC, 15- and 25-μm resolution 2DC gray, and 1D260X spectra in Fig. 3 are very similar. The 1D230X values used by NASA in their standard calibration are offset to significantly larger sizes (or higher concentrations), as they were for all runs at both tunnel velocities. In fact, the 1D230X-integrated LWC above 100 μm in Fig. 3 is more than 3 times that of the 2DC probe. Repeats for this and other test conditions reveal a high reproducibility (Fig. 3b), so that the differences cannot be explained by tunnel variability. Note the similar but smaller offset for the 2D2C in Fig. 3a, which again was persistent through all runs. Interestingly, a similar offset of about one channel in sizing between a 2D2C and 2DC was observed by Gayet et al. (1993), while their comparisons between several 2DC probes displayed smaller differences. Due to the fact that four OAPs in the present study provided quite similar results, it was decided that the most defendable approach was to use one of them to provide the intermediate-size drop spectrum component. The MSC 2DC was chosen because its size response has been characterized (Strapp et al. 2001). For the large particle part of the spectrum, the 1DP and 2DP were compared, and the 2DP was chosen because it provided a better overlap to the MSC 2DC probe. Interestingly, the NASA 1D230X and 1DP also smoothly overlap, albeit with the spectrum shifted to larger sizes relative to the 2DC and 2DP probes. The discrepancy between these two sets of probes is disturbing. Although efforts were made to trace the problem, the discrepancy remains unresolved.

The method used to construct the new composite spectra used in this article can be described as follows. PDPA concentrations were scaled by factors of 1.6 and 3.88 for 67 and 100 m s^{-1}, respectively, and the narrow size bins were combined into bins 2 μm wide. The PDPA data were used to form the smallest part of the size distribution between 2 and 62 μm. The MSC 2DC data were used for sizes above 62.5 μm (i.e., channels 3 and higher), and PDPA data above this size were discarded. The large-particle component of the spectrum was provided by the 2DP, above the diameter at which the 2DC stopped measuring particles due to insufficient sample volume (typically the second or third channel of the 2DP). Figure 4 displays the data from the three probes for test condition 17 (study MVD = 34.3 μm, 67 m s^{-1}). Note that the two lowest channels of the 2DC tend to underread relative to the PDPA, similar to the overlap behavior previously reported between the

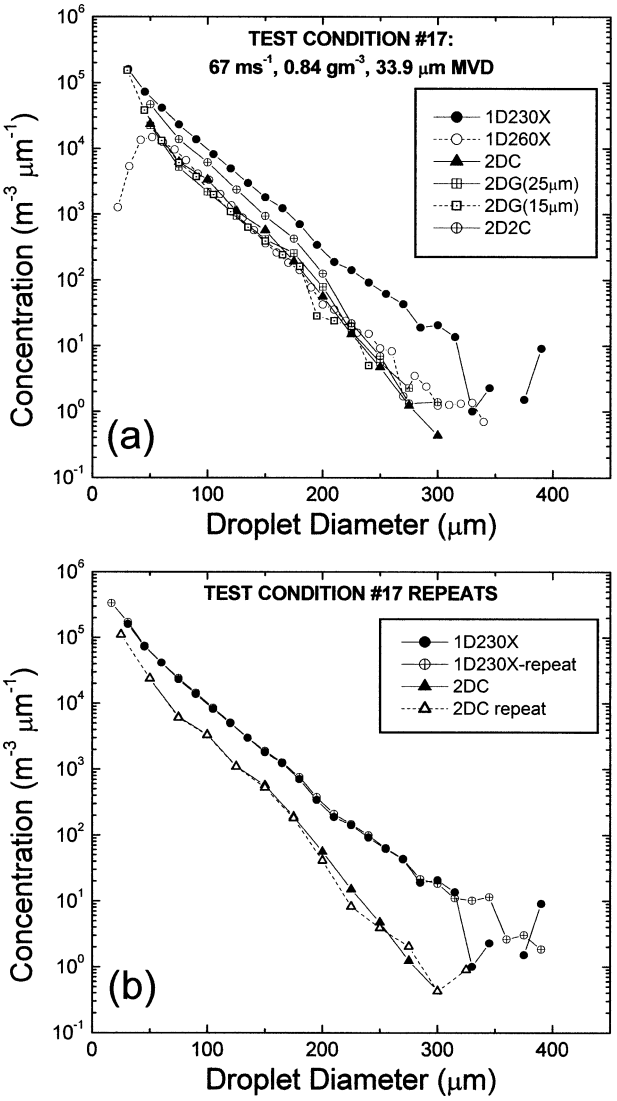

FIG. 3. Comparisons of different OAP spectra measured for test condition 17 (Table 2): (a) comparisons for all OAP cloud probes tested and (b) comparisons of repeats for the NASA 1D230X and the MSC 2DC probes.

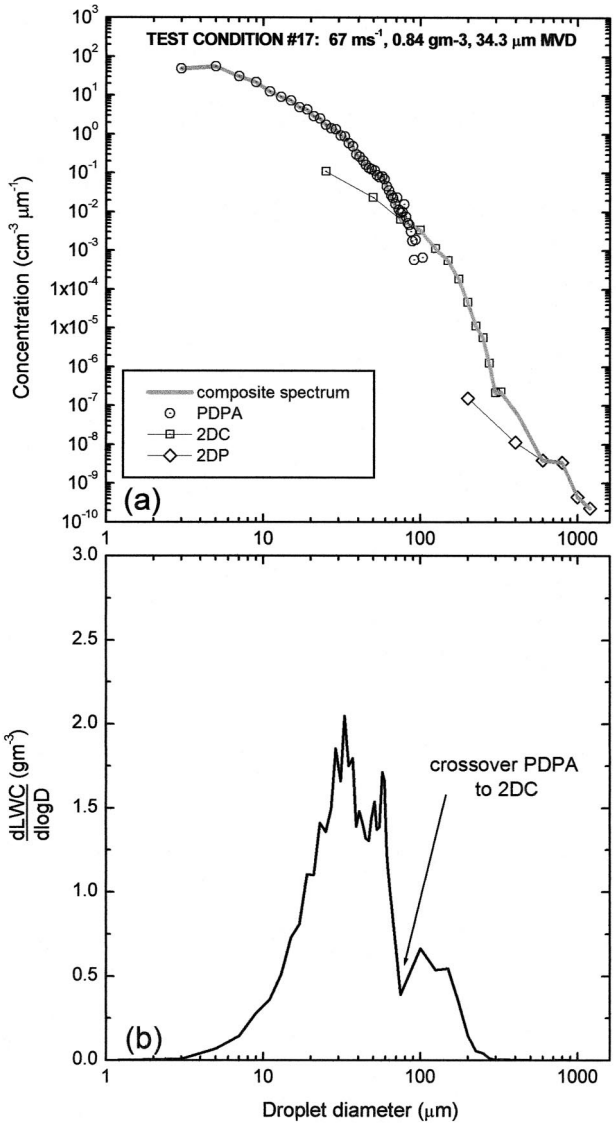

FIG. 4. Sample study composite spectrum for test condition 17 (Table 2): (a) particle number concentrations showing the individual PDPA, 2DC, and 2DP spectra, and the continuous composite spectrum formed from the three; and (b) the mass distribution for the composite spectrum shown in (a).

FSSPs and OAPs (e.g., Baumgardner and Korolev 1997). Figure 4 also reveals that the PDPA tends to roll off for large particle sizes (e.g., >75 μm) relative to the 2DC. For this reason, the composite spectrum was switched to the 2DC at 62.5 μm rather than the preferred 125-μm value, above which 2DC spectrum errors expressed as sizing errors are expected to drop below $\pm$10% if the probe sample time is accurately measured, and probe-produced artifacts are negligible (Strapp et al. 2001). Errors in the critical 50–100-μm region are unavoidable, since none of the probes in Table 1 are optimized for quantitative measurements in this size window.

Figures 5a–f display mass distributions for all MVD sweep test conditions at 67 m s^{-1}. One indication of the reliability of the composite distribution is the shape and continuity of the mass distribution at the probe crossover points. Distributions exhibit greater than 10% mass in the 2DC size region for study MVD larger than 30.8 μm (Figs. 5c–f). Most distributions display discontinuity features at the PDPA to 2DC crossover point, and simple bell-shaped distributions can be imagined to approximate the true distributions. The two strongest discontinuities are observed for the 50.8- and 57.0-μm MVD cases, where the true mode of the mass distribution is presumably in the problematic 50–100-μm size region noted above. Figure 5e also contains a rough estimate of a distribution smoothed to compensate for the discontinuity at the PDPA to 2DC crossover point in order to speculate on the associated error in MVD. A normal curve in log-diameter coordinates has been fitted by varying its mean and standard deviation until the errors in the regions <40 μm and >125 μm, which are believed to be covered accurately by the PDPA and 2DC, were minimized. The MVD for test condition 19 rises from 57 to 67 μm. Similarly, the MVDs for test conditions 17 and 18 rise from 33.9 to 36.7 and from 50.8 to 58.5, respectively. Figure 6 contains a comparison of new composite spectrum integrated LWC to the tunnel reference LWC for the test conditions of the 67 m s^{-1} MVD sweep. The ratios of composite spectrum LWC to tunnel reference LWC lie between 0.75 and 1.4. The reasonable agreement to the tunnel LWC for the two highest MVD cases, even though most of the LWC is in the 2DC and 2DP size ranges, is an encouraging result, although a larger number of high MVD comparisons would have been desirable. Overall, these are surprisingly good results given potential errors in deriving mass from particle spectra. Similar mass distributions and LWC comparisons were found for the 100 m s^{-1} composite spectra.

Table 2 contains the full list of the study MVDs to be used in the analysis of section 4. Rigorous error estimates are not possible due to the lack of any true MVD reference standards, and due to incomplete characterization of the probes used to make the measurements. However, some speculative estimates are possible based on the available information and the data collected during this study. For SD study MVDs <33.9 μm, where >85% of the mass is distributed in the PDPA size range, errors are estimated at $\pm$10%, as suggested by the manufacturer. For LD study MVDs between 33.9 and 123.1 μm, normal curve fits to the LWC distribution suggest a probable general tendency for study MVDs to be underestimates due to probe overlap discontinuity. When added to the expected errors in the LWC distributions >125 μm and <40 μm used to fit the normal curves, MVD errors in this size region are estimated to reach $\pm$30% at a study MVD of 58 μm. For simplicity, the errors in the 33.9–128-μm MVD region are therefore roughly estimated at $\pm$30%, and MVDs are more

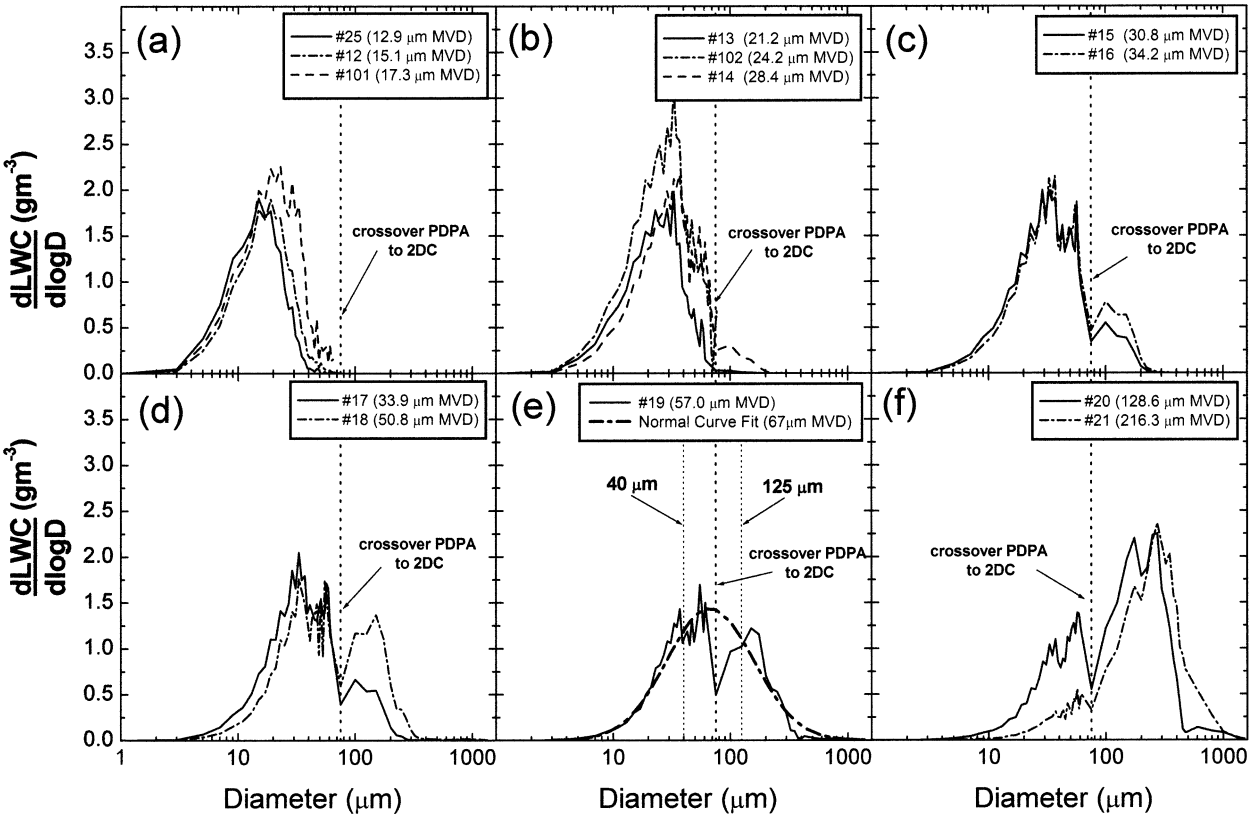

FIG. 5. Mass distributions for all 67 m s^{-1} MVD sweep test conditions (Table 2). A normal fit is shown in (e) as an example of a possible reconstruction of the poor crossover region of the PDPA to 2DC, particularly noticeable for test conditions 17–19.

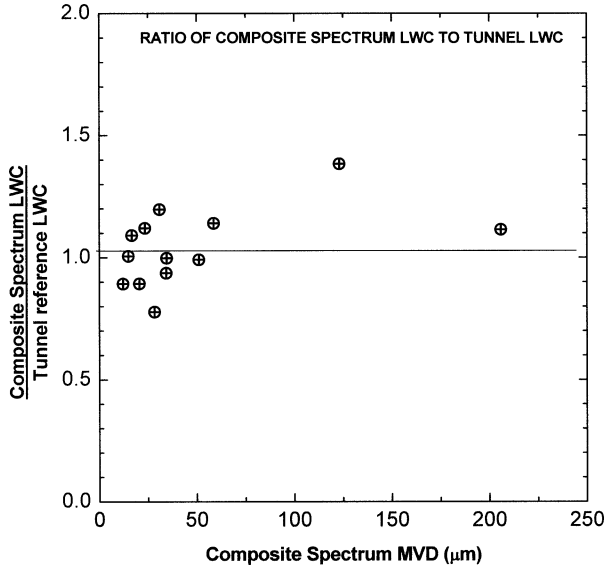

FIG. 6. Ratio of study composite spectrum integrated LWC to tunnel reference LWC for the 67 m s^{-1} MVD sweep (Table 2).

likely to be underestimates. In fact, some discontinuities observed in counterflow virtual impactor (CVI), icing blade, and icing cylinder response at the crossover from SD to LD LWCs are consistent with MVDs being underestimates in this size region. For the highest MVD test points above 200-μm MVD, where most of the LWC is above 125 μm, the results of Strapp et al. (2001) would suggest that spectrum error expressed as a sizing error, and thus the MVD error should be roughly $\pm 10\%$ assuming that 2D probe sample time is accurately measured and probe-produced artifacts are negligible. The error estimate has been increased here to $\pm 15\%$ to acknowledge the inevitability of other complicating factors. Overall, the errors in the integrated LWC of the composite spectra in Fig. 6 tend to imply that the MVD errors do not reach 30%. However, comparisons with the NASA MVDs reveal disagreement that is sometimes larger than the MVD error estimates. NASA and study MVDs for the 67 m s^{-1} MVD sweep (Table 2) agree to within 10% for study MVDs lower than about 28 μm, with the exception of a few low MVD points where high droplet concentrations may have biased NASA MVDs high due to FSSP coincidence oversizing. However, NASA MVDs greatly exceed study MVDs above 30 μm, with maximum discrepancies reaching 100% when the study MVDs are approximately 50 μm. The

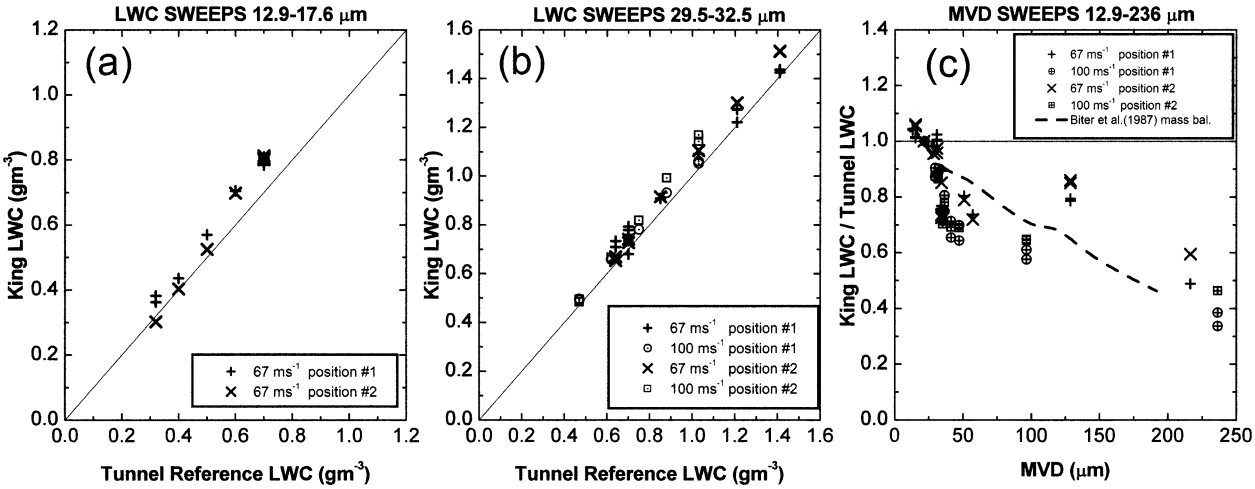

FIG. 7. PMS King hot-wire probe results: (a) comparisons of PMS King probe to tunnel reference LWCs for low MVD (12.9–17.6 μm) LWC sweeps (Table 2), (b) corresponding comparisons for the intermediate MVD (29.5–32.5 μm) LWC sweeps (Table 2), and (c) ratio of PMS King probe LWC to tunnel LWC as a function of study MVD, illustrating the probe response to increasing MVD. Results are shown for measurements in both primary positions in the tunnel.

largest MVD differences are largely due to the differences between the OAP measurements, where the NASA spectrum integrated LWC reaches a factor of 2 higher than the large icing cylinder reference LWC. This exercise has revealed the great difficulty in making MVD estimates in LD clouds and the difficulty in estimating the MVD errors. Up to three different instruments are required to cover the necessary size range, and the 50–100-μm part of the spectrum is particularly poorly measured by all probes. Biter et al. (1987) also observed large excesses in spectrum LWC relative to King probe measurements, using FSSP and 2DC gray probe to define their composite wind tunnel spectra.

4. Hot-wire results

Three hot-wire LWC probes and one hot-wire total water content probe were tested during this experiment (Table 1). The JW and the Nevzorov LWC/TWC sensors were each tested with two sets of electronics: standard electronics and new prototype electronics similar to those of the King probe. The prototype electronics for the JW and Nevzorov sensors were built by Science Engineering Associates (SEA) and MSC, respectively. Of particular interest here are the different cylindrical wire diameters and shapes of the various sensors, which as discussed earlier are expected to differently affect the inertial collision efficiency at smaller droplet sizes and the re-entrainment of water from the wire at larger droplet sizes. In order to minimize any effects introduced by differing probe electronics and focus primarily on wire shape effects, only the results from the JW and Nevzorov probes with the prototype King-type electronics will be presented.

In the next sections, the results for each hot-wire sensor will be described. The response of the probes as a function of MVD at quasi-constant LWC (Table 2, MVD sweeps) will be reported, as will the response of the probes as a function of LWC at low and intermediate MVDs (Table 2, LWC sweeps). The low MVD LWC sweep data at 100 m s^{-1} were problematic, with all hot wires and the airborne PVM-100A (Wendisch et al. 2002) showing a similar nonlinearity with tunnel LWC. The tunnel LWC calibration was re-examined, but no satisfactory explanation was found. Due to the similar response of multiple instruments, and the fact that such nonlinearity has never been observed with the PMS King probe in repeated previous and subsequent tunnel experiments at the NRC AIWT (e.g., King et al. 1985), it was decided to exclude the 100 m s^{-1} low MVD sweep data from the following analyses. In all cases, the data are 120-s averages centered in 150-s spray periods. Since all probes have drifting baselines, 10-s average values starting 15 s before and 5 s after each spray period have been averaged and subtracted from the total probe response. All data have been corrected for droplet–wire collision efficiency using the algorithm of Finstad et al. (1988), unless otherwise stated in the following sections.

a. PMS King probe results

The MSC King probe tested during this experiment had a wire diameter of 1.85 mm (outside diameter of wound wire) and a length of 19.95 mm, both measured during the experiment. These were measured under a magnifying lens with a precision caliper, with an estimated accuracy of ± 0.02 mm in diameter and ± 0.05 mm in length. The electronic gain of the circuit was also measured by directly comparing the output voltage to separate measurements across the 1-ohm resistor and the sensor wire. Figure 7a shows the comparisons of the

King LWC to the tunnel reference LWC for the 67 m s^{-1} low MVD LWC sweep. Data from the same King probe on two different days at both the primary test positions are shown. Note first that there are no significant differences between the two test positions given the overall LWC uncertainty described earlier. Almost all results indicate that the instrument readings exceed the tunnel reference LWC. The comparisons are quite linear, and the best fit through the origin suggests that the King probe exceeds tunnel reference values by approximately 13% (position 2) and 14% (position 1), both higher than the $\pm 5\%$ scale uncertainty suggested for the tunnel reference LWC. Figure 7b displays the corresponding results for the intermediate MVD LWC sweeps (29.5–32.5 μm), this time for both 67 and 100 m s^{-1}. Again, there are no large differences between the two test positions. The results are quite linear, and differences between the two airspeeds are very small. The slopes of the best-fit lines vary between 1.04 and 1.10, exceeding the reference LWC scale uncertainty of $\pm 5\%$ by a small amount. Figure 7c displays the ratio of the measured probe LWC to the tunnel reference LWC as a function of MVD, illustrating the rolloff in LWC with increasing drop size. In order to account for differing gains among the various probes in the following sections, the LWCs have been scaled by a factor close to unity so that the probe LWC is equal to the tunnel LWC at 20-μm MVD. This provides a graph that relates the measurement rolloff relative to the measurement at 20-μm MVD. The value of 20 μm was chosen because many previous LWC wind tunnel comparisons of hot-wire probes have been performed at 20-μm MVD (e.g., Strapp and Schemenaur 1982; King et al. 1985). In addition, inertial collision efficiencies have not been included in the hot-wire calculation of LWC for Fig. 7c, specifically to illustrate any signals in the data at SD sizes attributable to inertial collision efficiency, particularly important for the larger-diameter Nevzorov TWC probe. Note that the response of the probe is already dropping from the lowest MVD point at approximately 13 μm. At 50-, 100-, and 200-μm MVD, the response is approximately 70%, 60%, and 40% of the values at 20 μm, respectively. One strong outlier is observed for the test condition at 128-μm MVD, 67 m s^{-1}. This condition will repeatedly appears as an outlier in the other hot-wire calibrations and is most likely an error in the tunnel LWC calibration. Figure 7c suggests that the tunnel value might be approximately 30% high for this condition, if it were assumed to follow the general behavior of the other data points. The rolloff at 100 m s^{-1} appears to be a little stronger than at 67 m s^{-1}, although the differences can easily be explained by the combined uncertainty in the LWC and MVD measurements.

Biter et al. (1987) have also characterized the rolloff of the King probe as a function of MVD, using a PMS FSSP and a PMS 2DC gray probe to define the composite drop spectrum. Their mass-balance results, also shown in Fig. 7c, and again normalized to the response at 20-μm MVD, are quite similar to those of this study. One notable difference is that the dropoff in response for the current study is initially significantly stronger, particularly in the 25–50-μm MVD region, with the response at 50-μm MVD being approximately 70% relative to 20-μm MVD versus approximately 80% for Biter et al. (1987). The discrepancy may be due to uncertainties in the MVDs of either study. Biter et al. (1987) used similar instrumentation to derive their MVDs and reported significant difficulties in obtaining realistic masses in their composite spectra, concluding that the calibration procedures for these probes needed to be re-evaluated. They did not discuss the MVD uncertainties that these problems might entail.

b. Nevzorov LWC sensor measurements

The Nevzorov LWC utilizes the same size 1.8-mm cylindrical hot wire as the PMS King probe. However, in contrast to the fully exposed King wire, the Nevzorov LWC wire is mounted on the leading edge of a narrow vane, so that the trailing edge of the wire is not exposed. Nevertheless, the results of the Nevzorov LWC measurements (Figs. 8a–c) are quite similar to those reported above for the PMS King probe.

The low MVD LWC sweep comparison (Fig. 8a) reveals that the Nevzorov LWC overreads the tunnel reference LWC by about 12%, similar to the King results. At intermediate MVD, the response drop is a little stronger than in the case of the King probe, to about 96% of the tunnel LWC and with no airspeed dependency. The decrease in probe response with increasing MVD (Fig. 8c) reveals 70%, 60%, and 50% response relative to 20-μm MVD at 50-, 100-, and 200-μm MVD, respectively, probably insignificantly different from the values found for the King probe. As in the case of the King probe, the rolloff at 100 m s^{-1} appears a little stronger, and the 67 m s^{-1} point at 128-μm MVD appears as an outlier. Overall, the performance of the two probes is approximately the same.

c. Johnson–Williams sensor results

The JW system was tested with prototype electronics similar to a King probe, and a standard JW sensor head with a 0.56-mm solid nickel cylindrical sensor wire and a compensating wire oriented parallel to the flow to avoid wetting from droplets. The data from the compensating wire were not used in the subsequent analysis. The wire diameter of the JW is the smallest of the hot wires tested in this study.

The low MVD LWC sweep test (Fig. 9a) again displays results similar to the PMS King probe, with the JW reading about 12% higher than the tunnel reference LWC. However, the intermediate MVD sweep (Fig. 9b) shows a more significant response drop than the King and Nevzorov LWC probes, to about 80% of the tunnel

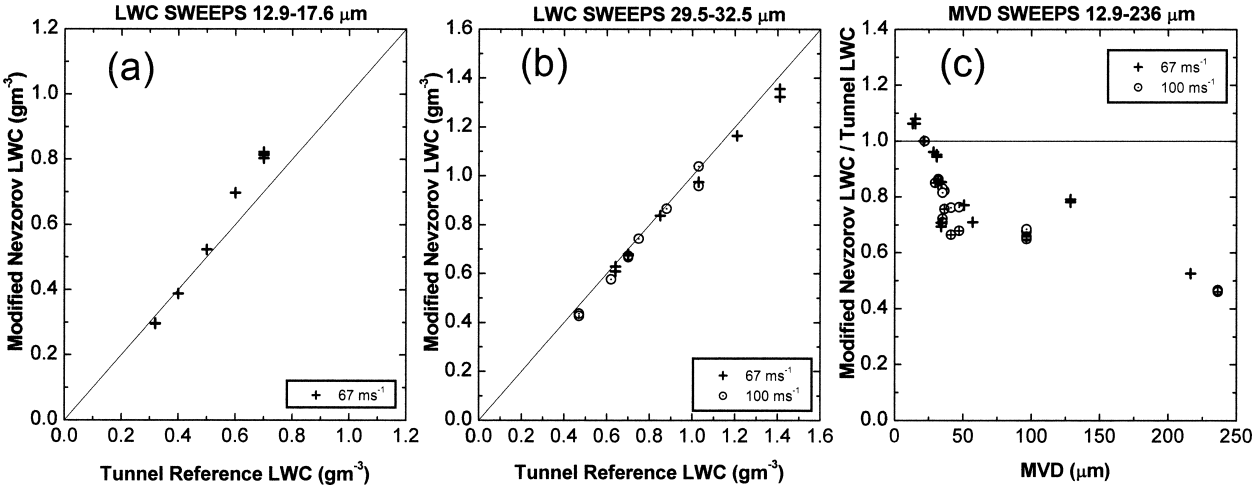

FIG. 8. As in Fig. 7, but for the ''modified'' Nevzorov LWC probe using a constant-temperature hot wire similar to that described by King et al. (1978). This probe was tested only in primary location 2, concurrently with the modified JW probe and the modified Nevzorov TWC probe.

values (linear regression slopes of 0.79 and 0.82 for 67 and 100 m s^{-1}, respectively). Note that as in the case of the PMS King probe, the response of the probe rolls off with increasing MVD, but at a faster rate than the King probe. At 50, 100, and 200 μm, the response of the probe relative to the 20-μm response is approximately 50%, 40%, and 25%, respectively, and the rolloff with drop size is a continuous effect that starts at MVDs at least as small as 13 μm. As in the case of the other probes, there is a weak indication that the rolloff at 100 m s^{-1} is a little stronger, and the 128-μm MVD point at 67 m s^{-1} is an outlier.

d. Nevzorov TWC sensor results

The Nevzorov TWC sensor is an 8-mm-diameter heated cone oriented into the airflow on the same sensor vane as the LWC sensor (Korolev et al. 1998b). When insignificant ice particle mass is present, as in the case of these experiments, the TWC measurement is equivalent to an LWC measurement. Figure 10 displays calculations of the collision efficiency of a two-dimensional shape simulating the side view of the Nevzorov TWC sensor for the two airspeed conditions of this study, as generated by the NASA LEWICE model (Wright 1995, 1999). These efficiencies are the best collision efficiency estimates available at this time and are used in the subsequent LWC sweep calculations. It is acknowledged that significant efficiency errors may exist, especially at small droplet diameters, and plans are under way to continue this work with a three-dimensional model. Previous experimentally derived estimates of the efficiency as a function of effective diameter (Korolev et al. 1998b) are also shown.

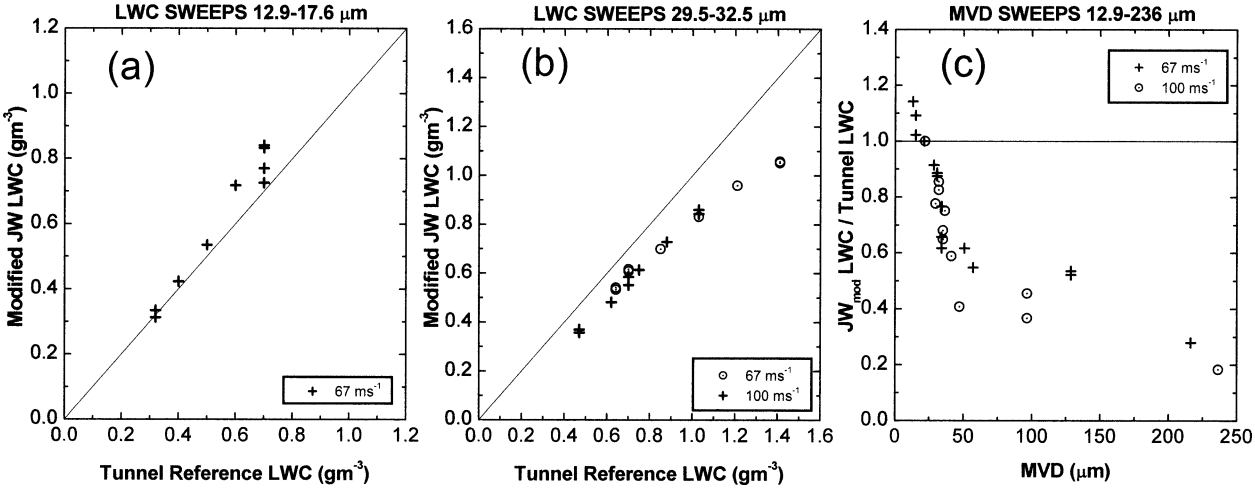

FIG. 9. As in Fig. 7, but for the ''modified'' JW probe using electronics similar to those described in King et al. (1978). This probe was tested only in primary location 1.

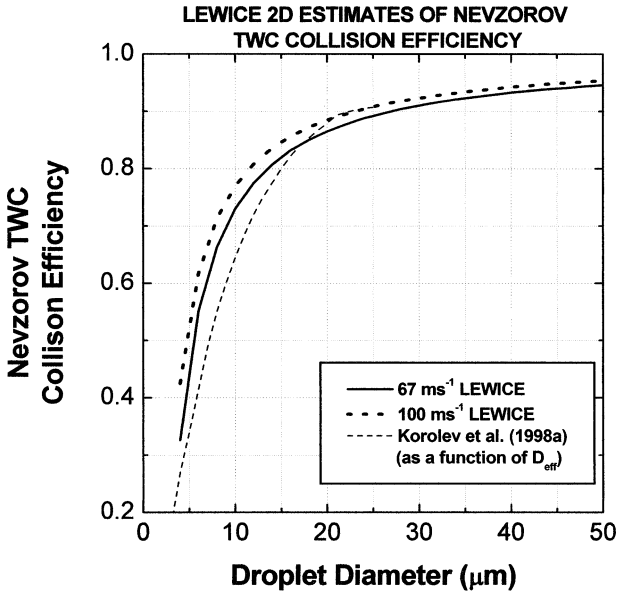

FIG. 10. Collision efficiency estimates for a 2D representation of the Nevzorov TWC sensor, using the NASA LEWICE model. The experimental results of Korolev et al. (1998b), as a function of effective diameter, are also shown.

The low MVD LWC sweep test (Fig. 11a) indicates that the TWC measurements are lower than tunnel reference values, with a slope value for the regression through the origin of 0.93. The discrepancy just exceeds the estimated scale error in the tunnel reference LWC of approximately $\pm 5\%$, and may be due to inaccuracies in the sample area estimate or, alternatively, could be due to errors in the collision efficiencies that are particularly important with these lower MVDs. Unlike the other probes, the comparisons to the tunnel are similar at the low and intermediate LWC sweeps, with regressions slopes for the latter of 0.95 and 0.99 for 67 and 100 m s^{-1}, respectively. Figure 11c displays the ratio of the measured probe LWC to the tunnel reference LWC as a function of spray MVD, again with all LWCs scaled so that ratio of probe LWC to tunnel LWC at 20 μm is 1.0, and with inertial collision efficiencies not applied in the LWC calculation. The change in probe response with increasing MVD is significantly different from that observed in the probes with cylindrical wires and supports the contention of Korolev et al. (1998b) that the TWC sensor inhibits droplet re-entrainment. Overall, there is no evidence of a rolloff in response to the probe for large droplets in the entire range of MVDs tested in this experiment (i.e., to nearly 250 μm). Many of the ratios are not significantly different from 1.0, given the $\pm 20\%$ uncertainty in the LWC estimated for the points with MVDs >34 μm, and the overall LWC uncertainty of about $\pm 12\%$ for individual points for MVDs <34 μm. The results are quite different from all of the other cylindrical sensors.

Figure 12 displays ratios of SEA JW LWC and Nevzorov LWC to the Nevzorov TWC for the 67 m s^{-1} MVD sweep. Although these data could be represented in several different ways, in this figure the simple instrument LWC output with no collision efficiency or gain adjustment has been used. The rolloff in the response of each probe with respect to the TWC measurements displays much less scatter than the corresponding ratios relative to the tunnel LWC (Figs. 8c and 9c). This is a direct indication of the extent of the scatter in these earlier figures due to the tunnel random fluctuations of LWC, which is eliminated in the direct simultaneous instrument comparisons of Fig. 12. The ratios of the cylindrical hot wires are larger than unity below about 30-μm MVD, a reflection of the lower collision efficiencies of the TWC sensor. The rolloff with increasing MVD is quite monotonic and well behaved for both wires, and the different behavior of the

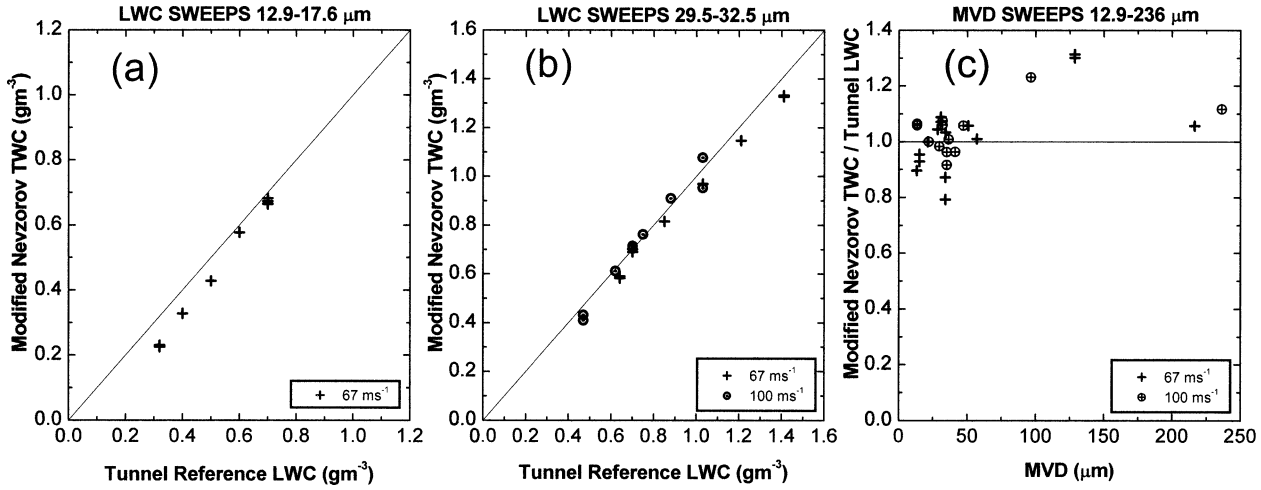

FIG. 11. As in Fig. 7, but for the ''modified'' Nevzorov TWC probe using electronics similar to those described by King et al. (1978). This probe was tested only in primary location 2, concurrently with the modified JW probe and the modified Nevzorov LWC probe.

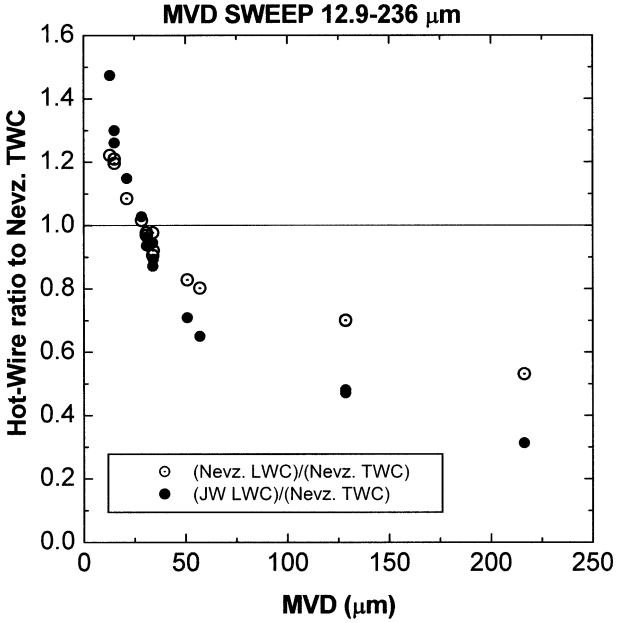

FIG. 12. Ratios of Nevzorov LWC and modified SEA JW LWC to Nevzorov TWC for the MVD sweep at 67 m s^{-1}. The probes were tested simultaneously.

two cylindrical wires is clear. The results suggests that if the relative gains of two independent systems with differing wire geometries such as those in Fig. 12 could be accurately maintained, then the MVD of clouds containing no significant ice fraction could be estimated directly from measurements from two or more physically different wires, if an initial calibration with respect to MVD could be established in a facility such as a wet wind tunnel. A prototype multiwire system is currently being developed by Science Engineering Associates specifically for this application.

5. Summary and conclusions

A series of wet wind tunnel tests was conducted at the NASA Icing Research Tunnel (IRT) to characterize the response of more than 23 instruments used for cloud LWC and droplet spectra measurements to liquid clouds with MVDs varying between approximately 13 and 236 μm. Tunnel LWC calibration references for the NASA IRT and the NRC Altitude Icing Wind Tunnel for small droplet conditions, the icing blade, and the small rotating icing cylinder, respectively, were compared to each other and to the NASA LWC parameterizations derived from earlier icing blade calibrations. Comparisons of icing blade measurements to the parameterizations showed an approximate $\pm$10% scatter indicative of the tunnel random fluctuations, but regression slopes suggested no change in the tunnel LWC calibration. Small icing cylinder LWCs were on the average approximately 4% higher than blade measurements, similar to the results of Stallabrass (1978), who also implied that the rotating icing cylinder should be accurate to within a few percent in absolute terms. The tunnel LWC is estimated to have an overall scale uncertainty of the order of $\pm$5% and a scatter dispersion for individual points of approximately 3.5%. The average absolute difference between repeats of icing blade measurements was 3.5%, with maximum differences of about $\pm$8%.

Measurement of MVD for sprays containing a significant mass of large droplets is difficult and involves the use of several probes with overlapping size regions. Rigorous error estimates are not possible due to the lack of any accepted comparison standards and incomplete characterization of the probes, and the attempts to estimate the MVD error for this study are complicated. The tunnel MVD has been previously characterized by NASA using PMS FSSP, 1D-230X, and 1DP probes. During the current tests, more than 10 different particle spectrometers were tested under the same matrix of test points, allowing for comparisons to the NASA results. The OAP comparisons showed disturbing and very significant consistent discrepancies. For this study, data from the PDPA, the MSC 2DC, and the MSC 2DP were used to form the composite drop spectra, and generate the quoted study MVDs. This particular combination of probes was chosen as most technically defendable, for a variety of reasons discussed earlier. The study MVD accuracy was roughly estimated at $\pm$10% in the 12.9–28.4-μm range, $\pm$30% in the 30.8–128.6-μm range, and $\pm$15% for the two test points above 200 μm. In the 30.8–128.6-μm range, the study MVDs are most likely to be underestimates. Although a defense for the use of 2DC probe measurements has been provided, if OAP comparison discrepancies are included in the accuracy estimates, the uncertainties rise significantly. For example, NASA and study MVD discrepancies tended to be larger than the above in some size regions, primarily due to differences between the MSC 2DC and the NASA 1D230X probes, a currently unresolved issue. The MVD estimate was thus found to be highly sensitive to the choice of instruments, leading to the natural speculation that large MVD biases probably exist between different icing tunnels, and between tunnel and aircraft measurements.

The response of four hot-wire probes with different sensor geometry to large droplets was characterized at 67 and 100 m s^{-1}. Constant wire-temperature electronics similar to the PMS King probe electronics were used in all cases, ensuring that differences could be attributed mainly to wire geometries. The three probes with cylindrical sensor wires all showed significant rolloff in LWC response with increasing droplet MVD, presumably due to re-entrainment of captured water before complete evaporation (Biter et al. 1987). The Johnson–Williams probe, with the smallest 0.56-mm wire diameter, displayed the strongest response rolloff. Approximately 50%, 40%, and 25% of the LWC, relative to 20-μm MVD, was measured at MVDs of 50, 100, and 200 μm, respectively. The response of the PMS

King probe was similar to the Nevzorov LWC probe, presumably due to their similar wire diameters of about 1.8 mm, with approximately 70%, 60%, and 45%, and 70%, 60%, and 50% measured (King and Nevzorov LWC, respectively) relative to 20-μm MVD at 50-, 100-, and 200-μm MVD. Results are similar to those of Biter et al. (1987) for the PMS King probe, although response rolloff is stronger in the current study, particularly in the 25–50-μm MVD interval. The Nevzorov TWC probe displayed much different results. All LWCs were within 30% of the tunnel values, and no rolloff in response with increasing MVD was observed. It is therefore evident that its relatively large-diameter conical sensor is superior to conventional small-diameter cylindrical hot wires for large-droplet cloud measurements, assuming that its higher small-droplet collision efficiency errors may be corrected using two-dimensional or preferably three-dimensional drop trajectory modeling results. This shape advantage results in the capture of ice particles as well as water droplets, a complicating factor that must also be considered in mixed-phase measurements. In all tests, response at both airspeeds was approximately the same. Ratios of measurements of the SEA Johnson–Williams and Nevzorov LWC probes to the Nevzorov TWC probe, for cases in which the probes were measuring simultaneously in the tunnel, revealed a quite monotonic and well-behaved rolloff with increasing MVD, leading to the speculation that the MVD of clouds with insignificant fractions of ice particle mass could be deduced directly from hot-wire measurements.

Acknowledgments. The authors would like to express their gratitude for the help of the NASA IRT operators and technicians, the technical help of Mohammed Wasey and Sergio Krickler of the Meteorological Service of Canada, and the expert probe calibration assistance of Frank Albers and Uwe Maixner of the GKSS, Germany. The NASA LEWICE calculations were kindly performed by William Wright. The National Center for Atmospheric Research loaned the PMS 1D260X probe used in these tests. Important advice on the use of the PDPA measurements was provided by W. Bachalo. Funding for this study was provided by the NASA Glenn Icing Branch, the Meteorological Service of Canada, the Federal Aviation Administration Technical Center, and Transport Canada.

REFERENCES

Baumgardner, D., and A. Korolev, 1997: Airspeed corrections for optical array probe sample volumes. *J. Atmos. Oceanic Technol.,* **14,** 1224–1129.

——, J. E. Dye, and J. W. Strapp, 1985: Evaluation of the Forward Scattering Spectrometer Probe. Part II: Corrections for coincidence and dead-time losses. *J. Atmos. Oceanic Technol.,* **2,** 626–632.

Biter, C. J., J. E. Dye, D. Huffman, and W. D. King, 1987: The drop-size response of the CSIRO liquid water probe. *J. Atmos. Oceanic Technol.,* **4,** 359–367.

Brenguier, J. L., 1989: Coincidence and dead-time corrections for particle counters. Part II: High concentration measurements with an FSSP. *J. Atmos. Oceanic Technol.,* **6,** 585–598.

——, and L. Amodei, 1989: Coincidence and dead-time corrections for particle counters. Part I: A general mathematical formulation. *J. Atmos. Oceanic Technol.,* **6,** 575–584.

——, D. Baumgardner, and B. Baker, 1994: A review and discussion of processing algorithms for FSSP concentration measurements. *J. Atmos. Oceanic Technol.,* **11,** 1409–1414.

Cooper, W. A., 1988: Effects of coincidence on measurements with a Forward Scattering Spectrometer Probe. *J. Atmos. Oceanic Technol.,* **5,** 823–832.

Finstad, K. J., E. P. Lozowski, and E. M. Gates, 1988: Computational investigation of water droplet trajectories. *J. Atmos. Oceanic Technol.,* **5,** 150–170.

Gayet, J.-F., P. R. A. Brown, and F. Albers, 1993: A comparison of in-cloud measurements obtained with six PMS 2D-C probes. *J. Atmos. Oceanic Technol.,* **10,** 180–194.

Ide, R. F., and J. R. Oldenburg, 2001: Icing cloud calibration of the NASA Glenn Icing Research Tunnel. *39th Aerospace Sciences Meeting and Exhibit,* Reno, NV, AIAA, AIAA 2001-0234.

Jensen, J. B., and H. Granek, 2002: Optoelectronic simulation of the PMS 260X optical array probe and application to drizzle in maritime stratocumulus. *J. Atmos. Oceanic Technol.,* **19,** 568–585.

King, W. D., D. A. Parkin, and R. J. Handsworth, 1978: A hot wire liquid water device having fully calculable response characteristics. *J. Appl. Meteor.,* **17,** 1809–1813.

——, J. E. Dye, J. W. Strapp, D. Baumgardner, and D. Huffman, 1985: Icing wind tunnel tests on the CSIRO liquid water probe. *J. Atmos. Oceanic Technol.,* **2,** 340–352.

Korolev, A. V., J. W. Strapp, and G. A. Isaac, 1998a: Evaluation of the accuracy of PMS optical array probes. *J. Atmos. Oceanic Technol.,* **15,** 708–720.

——, ——, ——, and A. N. Nevzorov, 1998b: The Nevzorov airborne hot-wire LWC–TWC probe: Principle of operation and performance characteristics. *J. Atmos. Oceanic Technol.,* **15,** 1495–1510.

Lawson, R. P., B. A. Baker, C. G. Schmitt, and T. L. Jensen, 2001: An overview of microphysical properties of Arctic clouds observed in May and July during FIRE ACE. *J. Geophys. Res.,* **106,** 14 989–15 014.

Merceret, F. J., and T. L. Schricker, 1975: A new hot-wire liquid cloud water meter. *J. Appl. Meteor.,* **14,** 319–326.

Neel, C. B., 1955: A heated-wire liquid-water-content instrument and results of initial flight tests in icing conditions. NASA Res. Memo. RM A54123, 33 pp.

Nevzorov, A. N., 1980: Aircraft cloud water content meter. *Proc. Eighth Conf. on Cloud Physics,* Vol. 2, Clermond-Ferrand, France, International Commission on Clouds and Precipitation, 701–703.

Oleskiw, M. M., F. H. Hyde, and P. J. Penna, 2001: In-flight icing simulation capabilities of NRC's Altitude Icing Wind Tunnel. *39th Aerospace Sciences Meeting and Exhibit,* Reno, NV, AIAA, AIAA 2001-0094.

Owens, G. V., 1957: Wind tunnel calibrations of three instruments designed for measurements of the liquid-water content of clouds. University of Chicago Cloud Physics Laboratory Tech. Note 10, 24 pp.

Reuter, A., and S. Bakan, 1998: Improvements of cloud particle sizing with a 2D-Grey probe. *J. Atmos. Oceanic Technol.,* **15,** 1196–1203.

Rudoff, R. C., E. J. Bachalo, and W. D. Bachalo, 1993: Liquid water content measurements using the Phase Doppler Particle Analyzer in the NASA Lewis Icing Research Tunnel. *31st Aerospace Sciences Meeting and Exhibit,* Reno, NV, AIAA, AIAA 1993-0298.

Spyers-Duran, P. A., 1968: Comparative measurements of cloud liquid water using heated wire and cloud replicating devices. *J. Appl. Meteor.,* **7,** 674–678.

Stallabrass, J. R., 1978: An appraisal of the single rotating cylinder

method of liquid water content measurement. National Research Council Canada, Rep. LTR-LT-92, 26 pp.

Strapp, J. W., and R. S. Schemenauer, 1982: Calibrations of Johnson–Williams liquid water content meters in a high-speed icing tunnel. *J. Appl. Meteor.,* **21,** 98–108.

——, F. Albers, A. Reuter, A. V. Korolev, U. Maixner, E. Rashke, and Z. Vukovic, 2001: Laboratory measurements of the response of a PMS OAP-2DC. *J. Atmos. Oceanic Technol.,* **18,** 1150–1170.

Twohy, C. H., W. J. Strapp, and M. Wendisch, 2003: Performance of a counterflow virtual impactor in the NASA Icing Research Tunnel. *J. Atmos. Oceanic Technol.,* **20,** 781–790.

Wendisch, M., T. J. Garrett, and J. W. Strapp, 2002: Wind tunnel tests of the airborne PVM-100A response to large droplets. *J. Atmos. Oceanic Technol.,* **19,** 1577–1584.

Wright, W. B., 1995: User's manual for the improved NASA Lewis Ice Accretion Code LEWICE 1.6. NASA Contractor Rep. 198355, 96 pp.

——, 1999: User manual for the NASA Glenn ice accretion code LEWICE version 2.0. NASA Contractor Rep. 1999-209409, 182 pp.